Structure-Guided Design of a High Affinity Platelet Integrin αIIbβ3 Receptor Antagonist That Displaces Mg^{2+} from the β3 MIDAS

Supplementary Materials and Methods

Materials: RUC-1, the inactive piperidine derivative of RUC-1, mAbs AP5 (a generous gift of Dr. Peter Newman, BloodCenter of Wisconsin), 10E3, and 7E3, tirofiban, and eptifibatide were obtained as previously described. The αIIbβ3 activating mAb PT25-2 was a generous gift of Dr. Makoto Handa of Keio University, Tokyo, Japan (*1*). n-octyl-β-D-glucoside (OG), 1,2-dimyristoyl-sn-glycero-3-phosphocholine (DMPC), and 1,2-dimyristoyl-sn-glycero-3-phospho-(1'-rac-glycerol) (DMPG) were purchased from Anatrace (Maumee, OH). Prostaglandin E_1 (PGE_1), isopropyl β-D-1-thiogalactopyranoside, α-methyl glucoside, leupeptin, uranyl acetate, and Triton X-100 were purchased from Sigma (St. Louis, MO, USA). Con A-Sepharose, Q-Sepharose, Nickel-Sepharose, Sephacryl S300, Superdex 200HR, and NHS-activated Sepharose were purchased from GE Healthcare (Piscataway, NJ). Bio-Bead SM-2 was purchased from Bio-Rad (Hercules, CA). PAC-1 was purchased from BD Biosciences (San Diego, CA) and 400 mesh carbon-coated copper grids were purchased from Electron Microscopy Sciences (Hatfield, PA).

General Synthetic Methods: Samples were analyzed for purity on an Agilent 1200 series LC/MS using a Zorbax Eclipse XBD-C8 reverse phase (5 micron, 4.6 x 150mm) column and a 1.1 mL/min flow rate. A gradient was performed using an acetonitrile/water mobile phase (each containing 0.1% trifluoroacetic acid). The gradient was 4% to 100% acetonitrile over 7 minutes and purity of final compounds was determined using a two microliter injection with quantitation by AUC at 220 and 254 nanometers. Chromatography on silica gel was performed

using forced flow (liquid) of the indicated solvent system on Biotage KP-Sil prepacked cartridges and using the Biotage SP-1 automated chromatography system. ^{1}H-spectra were recorded on a Varian Inova 400 MHz spectrometer. Chemical shifts are reported in ppm with the solvent resonance as the internal standard ($CDCl_3$ 7.26 ppm and DMSO-d_6 2.5 ppm). High resolution mass spectral data was collected in-house using an Agilent 6210 time-of-flight mass spectrometer, also coupled to an Agilent Technologies 1200 series HPLC system.

Synthesis of RUC-2: To a solution of 5-(3-nitrophenyl)-1,3,4-thiadiazol-2-amine (**2**) (3.0 g, 13.50 mmol) in MeCN (120 mL) was added methyl 3-chloro-3-oxopropanoate (1.735 mL, 16.20 mmol). The mixture was stirred at room temperature for 2 h. After consumption of the starting material, $POCl_3$ (60 mL, 644 mmol) was added along with DIPEA (2.358 mL, 13.50 mmol) in MeCN (10 mL). The mixture was heated in the microwave at 150 °C for 25 min, cooled, and concentrated *in vacuo.* The resulting slurry was taken up in chloroform, poured over ice and washed with saturated $NaHCO_3$, water and brine, dried over $MgSO_4$, and concentrated *in vacuo* to give a dark red oil which was purified via column chromatography on a 100 g snap column with 0-10% EtOAc/DCM gradient elution to give 7-chloro-2-(3-nitrophenyl)-5H-[1,3,4]thiadiazolo[3,2-a]pyrimidin-5-one (**3**) (1.36 g, 4.41 mmol, 32.6 % yield) as an orange solid. To a solution of 7-chloro-2-(3-nitrophenyl)-5H-[1,3,4]thiadiazolo[3,2-a]pyrimidin-5-one (**3**) (1.0 g, 3.24 mmol) in MeCN (30 ml) in a microwave vial was added *tert*-butyl 1-piperazinecarboxylate (0.724 g, 3.89 mmol) followed by DIPEA (1.697 ml, 9.72 mmol). The mixture was heated in the microwave at 150 °C for 25 min., cooled and concentrated *in vacuo* and purified via column chromatography on a 50 g snap column with 0-10% MeOH/DCM gradient elution to give tert-butyl 4-(2-(3-nitrophenyl)-5-oxo-5H-[1,3,4]thiadiazolo[3,2-a]pyrimidin-7-yl)piperazine-1-carboxylate (**4**) (1.44 g, 3.14 mmol, 97 % yield) as a tan solid. To

a solution of tert-butyl 4-(2-(3-nitrophenyl)-5-oxo-5H-[1,3,4]thiadiazolo[3,2-a]pyrimidin-7-yl)piperazine-1-carboxylate (**4**) (769 mg, 1.677 mmol) in EtOH (12 ml) at room temperature was added Raney(R) 2400 nickel (98 mg, 1.677 mmol) followed by hydrazine (0.526 ml, 16.77 mmol) dropwise. The mixture was stirred at room temperature for 4 hours. The reaction was monitored by TLC and LC/MS and additional nickel and hydrazine were added until the starting material disappeared. The mixture was filtered over celite and concentrated *in vacuo* to give crude tert-butyl 4-(2-(3-aminophenyl)-5-oxo-5H-[1,3,4]thiadiazolo[3,2-a]pyrimidin-7-yl)piperazine-1-carboxylate (**5**) (443 mg, 1.034 mmol, 61.6 % yield) as a tan solid. Crude tert-butyl 4-(2-(3-aminophenyl)-5-oxo-5H-[1,3,4]thiadiazolo[3,2-a]pyrimidin-7-yl)piperazine-1-carboxylate (**5**) (60 mg, 0.140 mmol) was dissolved in DMF (1.5 mL). To this solution was added the Boc-glycine (37 mg, 0.210 mmol) then EDC (40.3 mg, 0.210 mmol). After stirring at room temperature for 24 hours, the mixture was taken up in water and ethyl acetate. The layers were separated and the aqueous layer was extracted with ethyl acetate. The combined organic extracts were then washed with water twice, then brine, dried over $MgSO_4$, and concentrated *in vacuo* to give a yellow solid which was purified via column chromatography with 2-7% MeOH/DCM gradient to give tert-butyl 4-(2-(3-(2-(tert-butoxycarbonylamino)acetamido)phenyl)-5-oxo-5H-[1,3,4]thiadiazolo[3,2-a]pyrimidin-7-yl)piperazine-1-carboxylate (crude material confirmed by LCMS analysis). The residue was dissolved in 2 mL of dichloromethane. To this solution trifluoroacetic acid (1 ml, 13.0 mmol) was added and the mixture was stirred for 18 hours. The solution was then concentrated *in vacuo* and washed with dichloromethane to give a crude yellow solid that was dissolved in methanol and purified by preparative HPLC to give 2-amino-N-(3-(5-oxo-7-(piperazin-1-yl)-5H-[1,3,4]thiadiazolo[3,2-a]pyrimidin-2-yl)phenyl)acetamide (RUC-2)(NCGC00183896-01)(**1**) (40

mg, 49%) as a tan solid after HPLC purification. ^{1}H NMR (400 MHz, DMSO-d_6) δ ppm 8.31 (s, 1 H), 7.86 (d, *J*=7.43 Hz, 1 H), 7.48 - 7.58 (m, 2 H), 5.38 (s, 1 H), 3.46 (br. s., 4 H), 3.29 (s, 2 H), 2.67 - 2.76 (m, 4 H); LCMS (electrospray), *m/z* 386.1 $(MH)^+$; HPLC: t_R = 2.70 min, UV_{254} = >95%. HRMS (ESI): *m/z* calcd for $C_{17}H_{20}N_7O_2S$ $[M+H]^+$ 386.1394, found 386.1393. RUC-2 was synthesized as both the free base and a trifluoroacetic acid salt. The free base was soluble in water at concentrations up to 90 μM and in 10% DMSO in water at concentrations up to 1 mM.

Purification of integrin αIIβ3: αIIbβ3 was purified from outdated single donor platelet concentrates obtained from the New York Blood Center by washing platelets in the presence of PGE_1; removing contaminating blood cells by centrifugation; lysing the resuspended platelets at 4^oC in 5% (w/v) n-octyl-β-D-glucoside (OG) in 150 mM NaCl, 20 mM HEPES, 1 mM $CaCl_2$, 1 mM $MgCl_2$, 10 μM leupeptin, pH 7.4; performing concanavalin A affinity chromatography [binding buffer: 150 mM NaCl, 1% (w/v) OG, 20 mM HEPES, 1 mM $CaCl_2$, 1 mM $MgCl_2$, pH 7.4; washing buffer: binding buffer + 20 mM α-methyl glucoside; elution buffer: binding buffer + 1M α-methyl glucoside]; performing heparin affinity chromatography; applying the flow through fraction to Q-Sepharose [binding buffer: 75 mM NaCl, 1% (w/v) OG, 10 mM HEPES, 1 mM $CaCl_2$, 1 mM $MgCl_2$, pH 7.4; washing buffer: binding buffer + 200 mM NaCl; elution buffer: binding buffer + 400 mM NaCl]; and performing gel size exclusion chromatography on Sephacryl S300 HR [running buffer: 150 mM NaCl, 1% (w/v) OG, 10 mM HEPES, 1 mM $CaCl_2$, 1 mM $MgCl_2$, pH 7.4].

Preparation of αIIbβ3-containing nanodiscs: αIIbβ3-containing nanodiscs were prepared by a modification of the techniques described by Ritchie et al., Babyurt and Sligar, and Ye et al. (*2-4*). A full description is being reported separately. In brief, the His-tagged membrane scaffold protein was prepared as a recombinant protein in E. coli and purified by Ni affinity

chromatography and anion exchange chromatography. Final assembly consisted of solubilizing an equimolar mixture of 1,2-dimyristoyl-sn-glycero-3-phosphocholine and 1,2-dimyristoyl-sn-glycero-3-phospho-(1'-rac-glycerol) in octylglucoside and cholate and then adding the purified αIIbβ3. The detergents were removed with macroporous polymeric beads (Bio-Bead SM-2) and then the αIIbβ3 nanodiscs were separated from the empty nanodiscs by gel filtration.

Negative staining electron microscopy and evaluation of αIIbβ3 nanodisc particle size: αIIbβ3 nanodiscs were treated with eptifibatide, tirofiban, RUC-1, or RUC-2 for 1 hour at room temperature at the concentrations indicated in the text. Samples were loaded onto carbon-coated copper grids that were glow-discharged by a carbon coating unit (Edwards; Crowley, UK) and then stained with 2% uranyl acetate, followed by drying. Imaging of αIIbβ3 nanodiscs was performed using a JEOL JEM 100CX transmission electron microscope (Jeol Ltd; Tokyo, Japan) at 80 kV and magnifications of 33,000X and 50,000X. Individual nanodiscs containing αIIbβ3 were manually selected for analysis using Image J (NIH, Bethesda, MD). The distance from the bottom of the nanodisc to the height of the αIIbβ3 complex (nanodisc-integrin length; NIL) was measured as an indicator of integrin extension. The frequency distribution of NIL values was then analyzed for untreated αIIbβ3 nanodiscs and αIIbβ3 nanodiscs in the presence of different compounds.

Platelet function assays: The following assays were all carried out as previously described (*5*, *6*): platelet and HEK293 cell adhesion to fibrinogen; platelet adhesion/aggregation on collagen; platelet aggregation to ADP (5 μM); binding of fluorescent fibrinogen to platelets in the presence of the activating mAb PT25-2; binding of the αIIb-specific (PMI-1) and β3-specific (AP5 and LIBS1) LIBS mAbs to platelets; HEK293 cell αVβ3-mediated adhesion to vitronectin; and Stokes radius determination by chromatography and dynamic light scattering.

Protein expression, purification and crystallography: The expression, purification, and crystallization of the αIIbβ3 headpiece (αIIb β-propeller, thigh, and calf-1 domains and β3 β1, hybrid, PSI, and IEGF-1 domains) in complex with 10E5 Fab were performed as previously described (*6*). RUC-2 was soaked into the αIIbβ3/Fab crystals at 37.5 μM in the crystallization well solution containing 1 mM Ca^{2+} and 5 mM (or 20 mM) Mg^{2+} for 3-5 days. Crystals were harvested in 15% PEG 8000, 0.2 M ammonium sulfate, 0.1 M Tris-HCl, pH 8.9 plus 1 mM Ca^{2+} and 5 mM (or 20 mM) Mg^{2+} and cryoprotected with additional glycerol in 5% increments up to a 20% final concentration, and then flash frozen in liquid nitrogen. Diffraction data collected at ID-23 of APS was solved using molecular replacement. Final refinement with Phenix utilized translation-libration-screw (TLS) and noncrystallographic symmetry (NCS) analyses.

Gel filtration and dynamic light scattering (DLS): The purified $\alpha_{IIb}\beta_3$ headpiece at 2.0 μM was incubated with RUC-1, RUC-2, or tirofiban at 500 μM, 100 μM, and 56 μM, respectively, at 25ºC for 1h and subjected to Superdex 200 chromatography in Tris-buffered saline plus 1 mM Ca^{2+}/Mg^{2+}. DLS of the purified $\alpha_{IIb}\beta_3$ headpiece alone at 20 μM or after mixing with RUC-1, RUC-2, or tirofiban at 500 μM , 100 μM, and 56 μM, respectively, were measured at 25ºC using a Viscotek 802 DLS (Viscotek Corporation) in Tris-buffered saline plus 1 mM Ca^{2+}/Mg^{2+}.

Molecular docking: The crystal structure of the αIIbβ3 headpiece co-crystallized with the inhibitor RUC-1 (*5-7*) was used for the docking of RUC-2 (PDB code 3NIF). After RUC-1 was removed from the structure, RUC-2 docking was performed in the absence of the MIDAS Mg^{2+} ion. The SyMBS and ADMIDAS Ca^{2+} metal ions were retained, as were the crystallographic waters around the ions and the two water molecules close to Asp232. In the latter case, only the MIDAS Mg^{2+} was removed.

Prior to RUC-2 docking, a thorough exploration of the conformational space accessible to the ligand was performed. Specifically, about 3,000 conformations of RUC-2 were obtained using the program OMEGA version 2.3.2 (OpenEye Scientific Software, Santa Fe, NM). The semi-empirical quantum chemistry program AMSOL version 7.0 (Department of Chemistry and Supercomputing, University of Minnesota, Minneapolis, MN) was used to calculate partial atomic charges and transfer free energies.

Docking calculations of RUC-2, with its primary amine either uncharged or positively charged were performed with DOCK 3.5.54 (*8, 9*). Forty-five matching spheres, labeled for chemical matching based on the local receptor environment, were used to replace the atoms of the crystallographic ligand RUC-1. An energy-based score corresponding to the sum of the receptor-ligand electrostatic and van der Waals interaction energies corrected for ligand desolvation were assigned to each conformation. The best scored conformations of RUC-2 maintaining the same stable interactions of RUC-1(*6*) within the αIIbβ3 binding site received 100 steps of rigid-body energy minimization prior to further optimization using standard molecular dynamics (MD) simulations.

Molecular Dynamics (MD) simulations: The MD simulations of the selected complexes of αIIbβ3 with RUC-2 bound in a similar fashion to RUC-1 were carried out on truncated forms of the protein system (i.e., αIIb residues 1-452 and β3 residues 108-352) using the AMBER10.0 suite of programs (http://ambermd.org/). The initial geometry of RUC-2 was optimized *ab initio* using a restricted Hartree-Fock (RHF) method and a 6-31G (d) basis set, as implemented in the Gaussian 03 program (*10*), and previously calculated RESP point charges (*5*, *6*). The bonded and non-bonded RUC-2 parameters were automatically assigned using the general AMBER force field (GAFF) for organic molecules (*11*). Each molecular system was neutralized by the addition

of seven or five sodium ions (*12*), and immersed in a rectangular box of ~22,500 TIP3P water molecules. Periodic boundary conditions and the NPT ensemble (constant pressure and temperature) were applied during the MD simulations. Electrostatic interactions were treated using the smooth Particle Mesh Ewald (PME) method (*13*) with a grid spacing of 1 Å. The cutoff distance for the nonbonded interactions was set to 9 Å. The SHAKE algorithm (*14*) was applied to all bonds, and an integration step of 2.0 fs was used. Solvent molecules and counterions were first relaxed by energy minimization and then allowed to redistribute around positionally restrained protein–ligand complexes (25 kcal mol^{-1} $Å^{-2}$) during 0.1 ns. The initial positional restraints were increasingly reduced in a series of four relaxation runs of 0.1 ns each until they were completely removed. The resulting systems were allowed to equilibrate in the absence of any restraints for 10 ns during which system coordinates were collected every 2 ps for further analysis, as previously described (*6*). The molecular visualization package PyMOL was used to visually inspect representative snapshots.

Detection of antibodies from patients with tirofiban- or eptifibatide-induced thrombocytopenia: To assess whether RUC-1 or RUC-2 induce conformational changes in αIIbβ3 similar to those produced by eptifibatide and tirofiban that result in recruitment of IgG to the platelet surface in patients who develop thrombocytopenia after treatment with one or the other drug, we used the assay described previously (*15*). In brief, 10 µl of patient serum diluted 1:5 was incubated with $5x10^6$ washed group O platelets (isolated from citrated whole blood and washed in the presence of PGE_1) together with tirofiban (4 µM), eptifibatide (2.4 µM), RUC-1 (100 µM), or RUC-2 (3.9 µM) in a total volume of 50 µl. After 1 hour at RT, platelets were washed twice in HEPES buffer containing the drug at the same concentration as in the primary mixture and suspended in 25 µl of HEPES buffer containing the drug at twice the concentration

used in the primary mixture and 25 µl of fluorescein-labeled anti-Ig antibody (heavy and light chain-specific), diluted 1:100. After incubation in the dark for 45 minutes, an aliquot was diluted in 0.1 ml buffer and platelet-bound fluorescence was analyzed by flow cytometry (FACScan, Becton-Dickinson). A "positive" reaction was defined as a median platelet fluorescence intensity (MFI) at least twice that of platelets treated identically in the absence of drug. This value always exceeded the value obtained with normal serum plus drug or patient serum in the absence of drug by at least three standard deviations.

Statistical analysis. Data are presented as mean ± SD. Group comparisons were performed by Student's t test. IC_{50} values for platelet aggregation data, which were expressed as a percentage of the control value in the absence of αIIbβ3 antagonist, were estimated from a two-parameter logistic function. The IC_{50} (e) was given by the logistic function:

$$f(x) = \frac{100}{1 + e^{b[log(x) - log(e)]}}$$

where b represents the slope. The drc (dose response curves) package from R open source software (www.R-project.org) was used to compute the IC_{50}s.

Supplementary Figure Legends

Fig. S1. Synthesis of RUC-2 (1) (NCGC00183896-01).

Fig. S2. Effect of RUC-1 and RUC-2 on the aggregation of citrated platelet-rich plasma from mice (**A**), rat (**B**), and transgenic mice expressing human α_{IIb} and mouse β_3 (**C**). RUC-1 was tested at 100 μM and RUC-2 at 1 μM. Aggregation was induced by ADP (30 μM for mouse and rat; 5 μM for human) in the absence of either compound (control) or in the presence of one or the other compound. Single representative tracings are presented.

Fig. S3. Effect of mAbs 6F1, 10E5, or 7E3, RUC-1, and RUC-2 on platelet adhesion to collagen. Rat skin type 1 collagen was immobilized on microtiter plates and washed platelets in buffer containing Mg^{2+} were allowed to adhere for 1 hour in the absence or presence of the mAbs 6F1, 10E5 or 7E3, RUC-1, RUC-2, or RUC-2 + 10E5 at the indicated concentrations.

Fig. S4. Effect of mAbs LM609 or 7E3, RUC-1, and RUC-2 on adhesion of HEK293 cells expressing $\alpha_V\beta_3$ to vitronectin and HEK293 cells expressing $\alpha_{IIb}\beta_3$ to fibrinogen. Cells expressing $\alpha_V\beta_3$ or $\alpha_{IIb}\beta_3$, respectively, were added to microtiter wells precoated with either vitronectin (5 μg/ml) or fibrinogen (50 μg/ml). After 1 hour, the wells were washed and cell adhesion measured by assaying endogenous acid phosphatase activity. mAb LM609 is specific for $\alpha_V\beta_3$ whereas mAb 7E3 reacts with both $\alpha_V\beta_3$ and $\alpha_{IIb}\beta_3$.

Fig. S5. Induction of ligand-induced binding site (LIBS) epitopes. The binding of the β3 antibodies AP5 and LIBS and the LIBS antibody PMI-1 were tested in the presence of eptifibatide (1 μM), RUC-1 (100 μM), and RUC-2 (1 μM). The net fluorescence intensity after

subtracting background binding was expressed as a percentage of the value in the presence of eptifibatide, the positive control.

Fig. S6. Ligand-binding pocket of $\alpha_{IIb}\beta_3$ headpiece crystal soaked with RUC-2 and 20 mM Mg^{2+}. (**A**) Molecule 1 of asymmetric unit. (**B**) Molecule 2 of asymmetric unit. 2Fo-Fc maps at 1.0 σ for water (red spheres), Cl^- ions (green spheres), Ca^{2+} ions (yellow sphere), and Mg^{2+} ion (silver sphere) are shown in blue. Selected side chains are shown as sticks with red oxygens and blue nitrogens.

Fig. S7. Results of the MD simulations of the RUC-2–$\alpha_{IIb}\beta_3$ fragment complexes in the absence of the MIDAS Mg^{2+} ion. (**A**) Representative snapshot from MD simulations of the RUC-2 (+1 charge)-αIIbβ3 fragment complex. (**B**) Representative snapshot from MD simulations of the RUC-2 (+2 charge)-αIIbβ3 fragment complex. (**C**) Minimum distance between either oxygen of the Glu-220 side chain and the nitrogen of the terminal, neutral amine of RUC-2. (**D**) Minimum distance between either oxygen of the Glu-220 side chain and the nitrogen of the terminal, charged amine of RUC-2.

Fig. S1

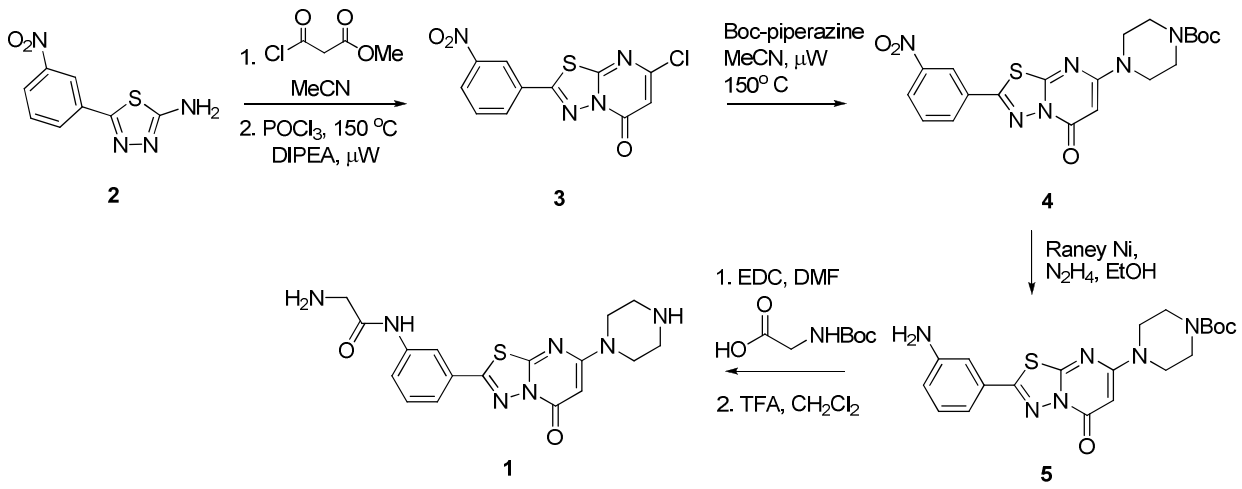

Abbreviations: MeCN, acetonitrile; $POCl_3$, phosphoryl chloride; DIPEA, *N*,*N*-diisopropylethylamine; μW, microwave; N_2H_4, cis-diazene; EtOH, ethyl alcohol; DMF, dimethyl formamide; TFA, tetrahydrofluoric acid; CH_2Cl_2, dichloromethane.

Fig. S2

A

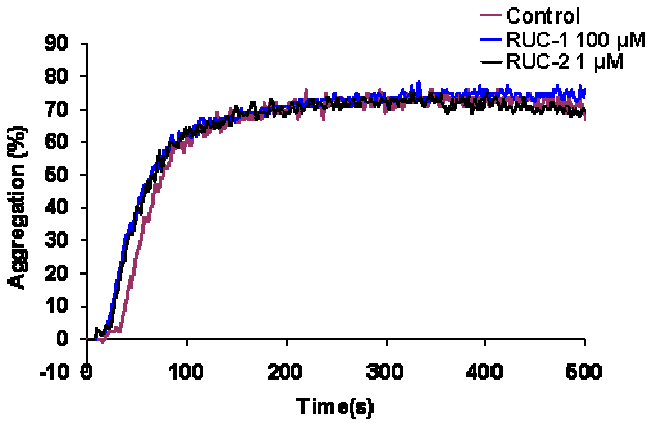
Control
RUC-1 100 μM
RUC-2 1 μM
Aggregation (%)
Time(s)

B

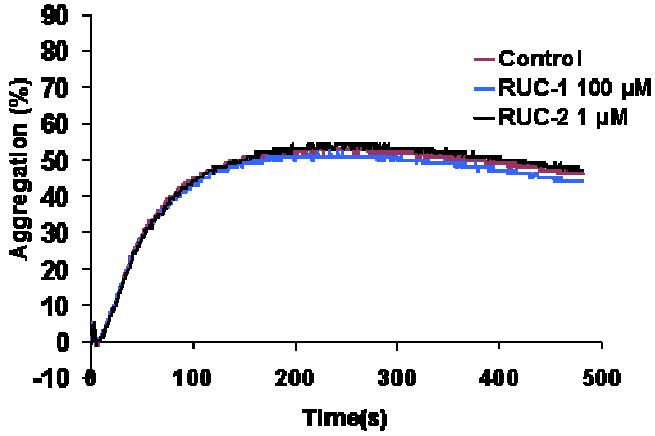
Control
RUC-1 100 μM
RUC-2 1 μM
Aggregation (%)
Time(s)

C

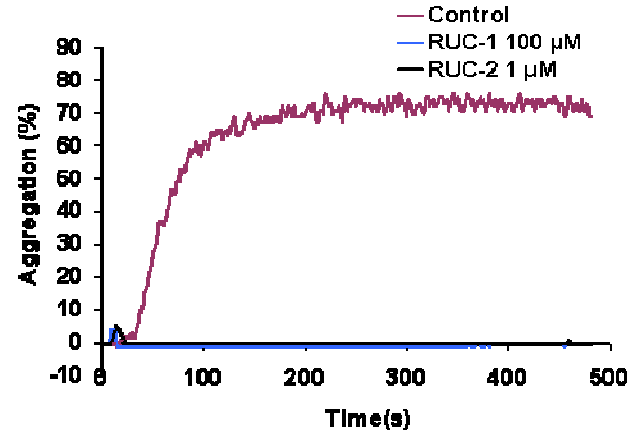
Control
RUC-1 100 μM
RUC-2 1 μM
Aggregation (%)
Time(s)

Fig. S3

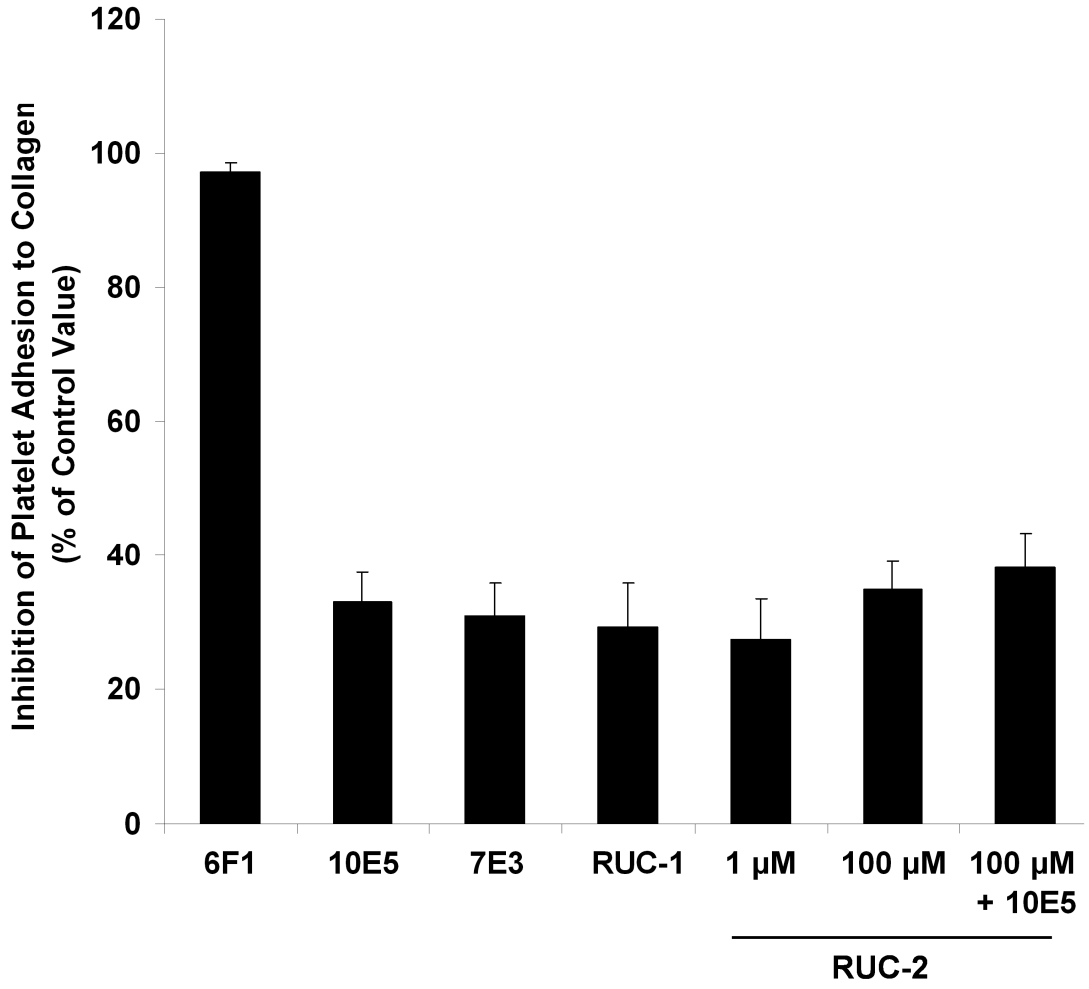
Inhibition of Platelet Adhesion to Collagen
(% of Control Value)
120
100
80
60
40
20
0
6F1
10E5
7E3
RUC-1
1 μM
100 μM
100 μM
+ 10E5
RUC-2

Fig. S4

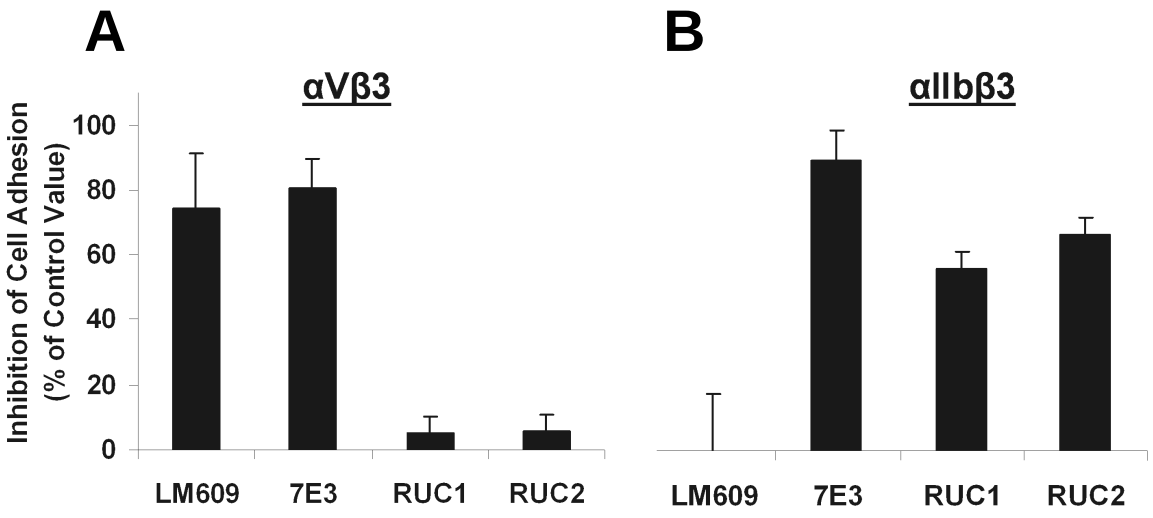
A
αVβ3
Inhibition of Cell Adhesion
(% of Control Value)
100
80
60
40
20
0
LM609
7E3
RUC1
RUC2
B
αIIbβ3
LM609
7E3
RUC1
RUC2

Fig. S5

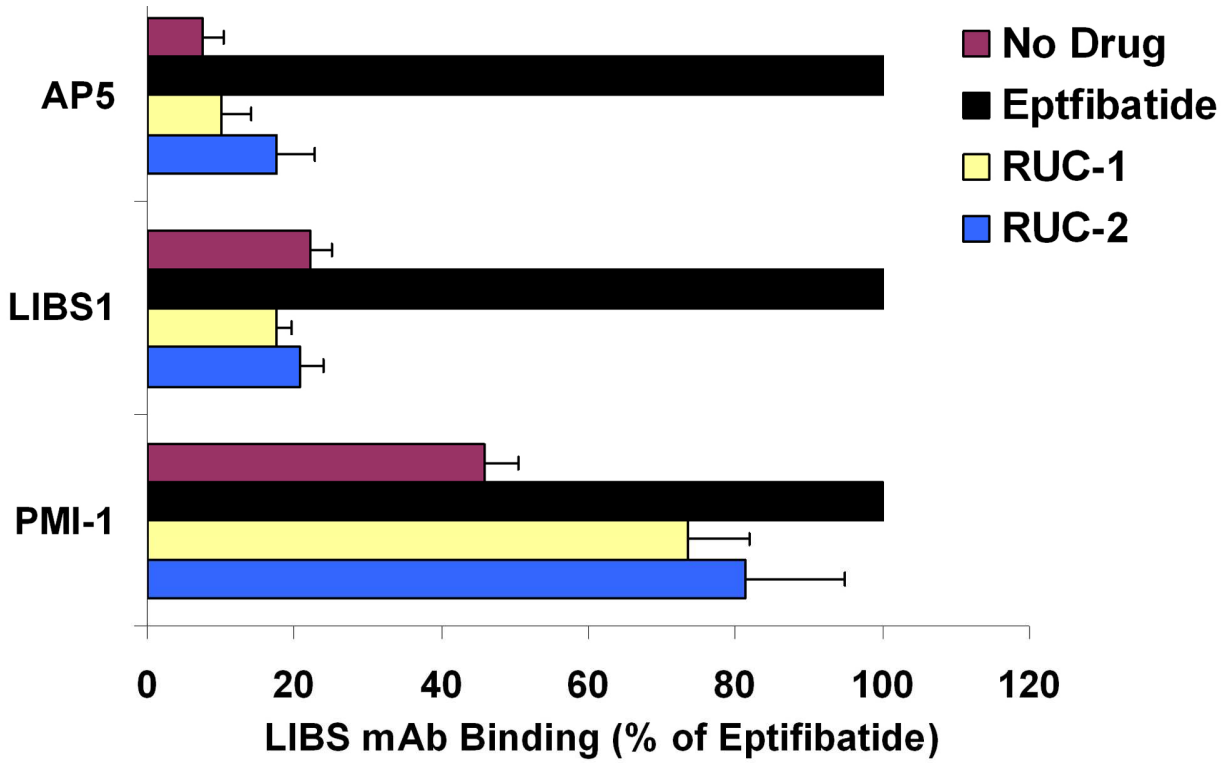
AP5
LIBS1
PMI-1
No Drug
Eptfibatide
RUC-1
RUC-2
0
20
40
60
80
100
120
LIBS mAb Binding (% of Eptifibatide)

Fig. S6

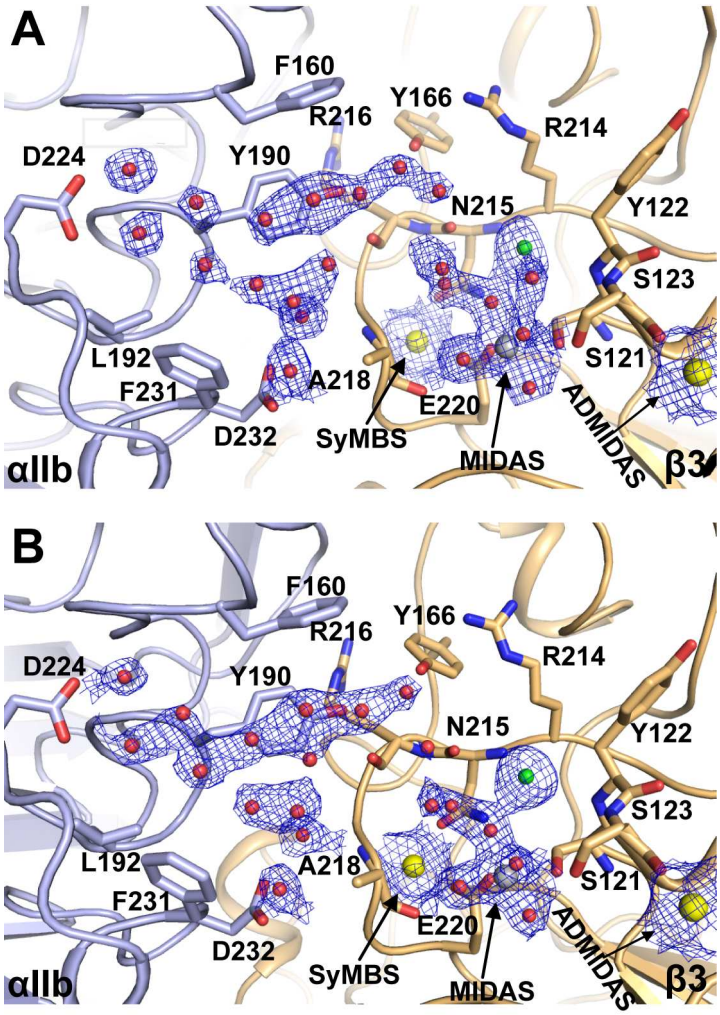
A
F160
R216
Y166
R214
D224
Y190
N215
Y122
S123
L192
F231
A218
E220
S121
D232
SyMBS
MIDAS
ADMIDAS
αIIb
β3
B
F160
R216
Y166
R214
D224
Y190
N215
Y122
S123
L192
F231
A218
E220
S121
D232
SyMBS
MIDAS
ADMIDAS
αIIb
β3

Fig. S7

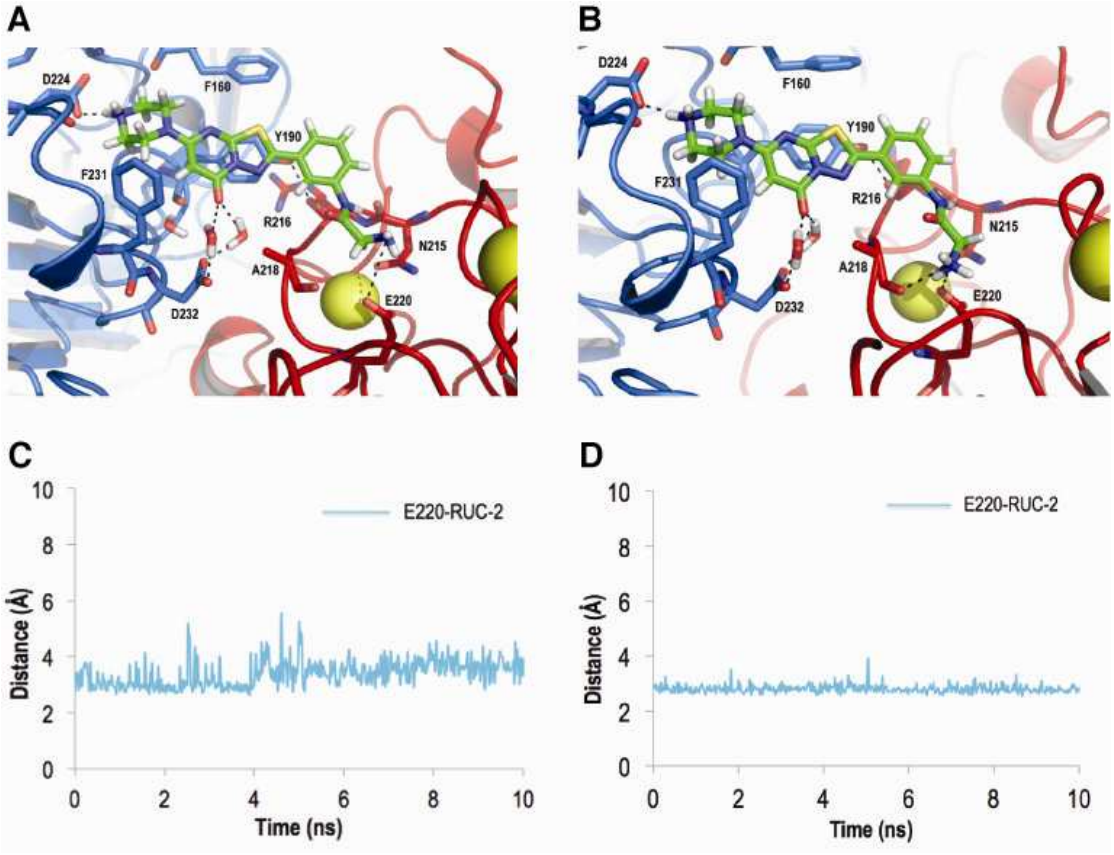
A
D224
F160
Y190
F231
R216
N215
A218
E220
D232
B
D224
F160
Y190
F231
R216
N215
A218
E220
D232
C
E220-RUC-2
Distance (Å)
Time (ns)
D
E220-RUC-2
Distance (Å)
Time (ns)

References

1. M. Tokuhira, M. Handa, T. Kamata, A. Oda, M. Katayama, Y. Tomiyama, M. Murata, Y. Kawai, K. Watanabe, Y. Ikeda, A novel regulatory epitope defined by a murine monoclonal antibody to the platelet GPIIb-IIIa complex ($\alpha_{IIb}\beta_3$ integrin). *Thromb. Haemost.* **76**, 1038–1046 (1996).
2. T. K. Ritchie, Y. V. Grinkova, T. H. Bayburt, I. G. Denisov, J. K. Zolnerciks, W. M. Atkins, S. G. Sligar, Reconstitution of membrane proteins in phospholipid bilayer nanodiscs. *Methods Enzymol.* **464**, 211–231 (2009).
3. T. H. Bayburt, S. G. Sligar, Membrane protein assembly into nanodiscs. *FEBS Lett.* **584**, 1721–1727 (2010).
4. F. Ye, G. Hu, D. Taylor, B. Ratnikov, A. A. Bobkov, M. A. McLean, S. G. Sligar, K. A. Taylor, M. H. Ginsburg, Recreation of the terminal events in physiological integrin activation. *J. Cell Biol.* **188**, 157–173 (2010).
5. R. Blue, M. Murcia, C. Karan, M. Jirouskova, B. S. Coller, Application of high-throughput screening to identify a novel αIIb-specific small-molecule inhibitor of αIIbβ3-mediated platelet interaction with fibrinogen. *Blood* **111**, 1248–1256 (2008).
6. J. Zhu, J. Zhu, A. Negri, D. Provasi, M. Filizola, B. S. Coller, T. A. Springer, Closed headpiece of integrin $\alpha_{IIb}\beta_3$ and its complex with an $\alpha_{IIb}\beta_3$-specific antagonist that does not induce opening. *Blood* **116**, 5050–5059 (2010).
7. R. Blue, M. A. Kowalska, J. Hirsch, M. Murcia, C. A. Janczak, A. Harrington, M. Jirouskova, J. Li, R. Fuentes, M. A. Thornton, M. Filizola, M. Poncz, B. S. Coller, Structural and therapeutic insights from the species specificity and in vivo antithrombotic activity of a novel αIIb-specific αIIbβ3 antagonist. *Blood* **114**, 195–201 (2009).
8. D. M. Lorber, B. K. Shoichet, Hierarchical docking of databases of multiple ligand conformations. *Curr. Top. Med. Chem.* **5**, 739–749 (2005).
9. E. C. Meng, B. K. Shoichet, I. D. Kuntz, Automated docking with grid-based energy evaluation. *J. Comp. Chem.* **13**, 505–524 (1992).
10. M. J. Frisch, G. W. Trucks, H. B. Schlegel, G. E. Scuseria, M. A. Robb, J. R. Cheeseman, J. A. Montgomery Jr., T. Vreven, K. N. Kudin, J. C. Burant, J. M. Millam, S. S. Iyengar, J. Tomasi, V. Barone, B. Mennucci, M. Cossi, G. Scalmani, N. Rega, G. A. Petersson, H. Nakatsuji, M. Hada, M. Ehara, K. Toyota, R. Fukuda, J. Hasegawa, M. Ishida, T. Nakajima, Y. Honda, O. Kitao, H. Nakai, M. Klene, X. Li, J. E. Knox, H. P. Hratchian, J. B. Cross, V. Bakken, C. Adamo, J. Jaramillo, R. Gomperts, R. E. Stratmann, O. Yazyev, A. J. Austin, R. Cammi, C. Pomelli, J. W. Ochterski, P. Y. Ayala, K. Morokuma, G. A. Voth, P. Salvador, J. J. Dannenberg, V. G. Zakrzewski, S. Dapprich, A. D. Daniels, M. C. Strain, O. Farkas, D. K. Malick, A. D. Rabuck, K. Raghavachari, J. B. Foresman, J. V. Ortiz, Q. Cui, A. G. Baboul, S. Clifford, J. Cioslowski, B. B. Stefanov, G. Liu, A. Liashenko, P. Piskorz, I. Komaromi, R. L. Martin, D. J. Fox, T. Keith, M. A. Al-Laham, C. Y. Peng, A. Nanayakkara, M. Challacombe, P. M. W. Gill, B. Johnson, W. Chen, M. W. Wong, C. Gonzalez, J. A. Pople, Gaussian 03, Revision C.02 (Gaussian, Inc., Wallingford, CT, 2004).
11. J. Wang, R. M. Wolf, J. W. Caldwell, P. A. Kollman, D. A. Case, Development and testing of a general amber force field. *J. Comput. Chem.* **25**, 1157–1174 (2004).
12. J. Aqvist, Ion-water interaction potentials derived from free energy perturbation simulations. *J. Phys. Chem.* **94**, 8021–8024 (1990).
13. T. A. Darden, D. York, L. G. Pedersen, Particle mesh Ewald: An *N*-log(*N*) method for Ewald sums in large systems. *J. Chemical Physics* **98**, 10089–10093 (1993).

14. J.-P. Ryckaert, G. Ciccoti, H. J. C. Berendsen, Numerical integration of the cartesian equations of motion of a system with constraints: Molecular dynamics of *n*-alkanes. *J. Computational Physics* **23**, 327–341 (1977).
15. D. W. Bougie, P. R. Wilker, E. D. Wuitschick, B. R. Curtis, M. Malik, S. Levine, R. N. Lind, J. Pereira, R. H. Aster, Acute thrombocytopenia after treatment with tirofiban or eptifibatide is associated with antibodies specific for ligand-occupied GPIIb/IIIa. *Blood* **100**, 2071–2076 (2002).